Environmental Science & Technology

pubs.acs.org/est

Article

Mode of Atmospheric Deposition in Forests Demonstrates Notable Differences in Initial Radiocesium Behavior

Donovan Anderson,* Hiroaki Kato, and Yuichi Onda*

Cite This: *Environ. Sci. Technol.* 2022, 56, 15541−15551

Read Online

ACCESS | Metrics & More | Article Recommendations | Supporting Information

ABSTRACT: The March 2011 Fukushima Dai-ichi Nuclear Power Plant accident in Japan released 520 PBq of radionuclides compared to a total release of 5300 PBq from the Chornobyl Nuclear Power Plant accident. Both nuclear accidents resulted in deposition of radiocesium throughout the northern hemisphere, and a plethora of studies have been performed regarding radiocesium (^{137}Cs) behavior. However, few studies have assessed the impact of precipitation on ^{137}Cs deposition in forests. Wide-scale environmental measurements from 2011 and 2016 were used to determine the differences in ^{137}Cs deposition because of precipitation following the Fukushima accident. In areas where wet deposition processes were dominant, dense forests generally had lower ambient dose rates and levels of contamination on forest floors than other stands with fewer stems per hectare in 2011. Similar tendencies were not observed in areas that were primarily subject to dry deposition nor were any trends observed in 2016. ^{137}Cs was retained in dense forest canopies for an extended period regardless of the deposition mode. Additionally, it was found that the initial retention of radionuclides by forest canopies is in general higher for areas with predominantly dry deposition. Incorporation of radiocesium into wood tissues was the same for both wet and dry deposition.

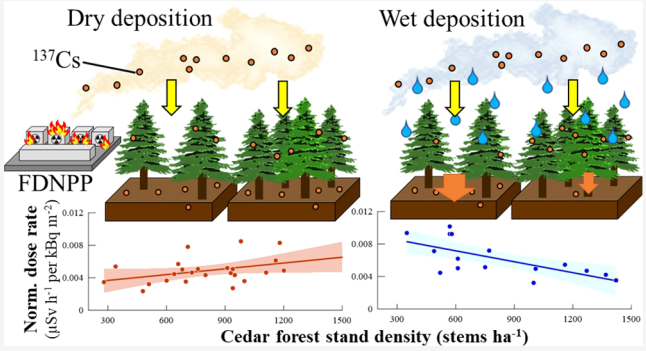

KEYWORDS: *dry and wet deposition, radiocesium, forest, Fukushima*

Downloaded via KU LEUVEN on July 17, 2025 at 12:22:23 (UTC).
See https://pubs.acs.org/sharingguidelines for options on how to legitimately share published articles.

■ INTRODUCTION

A catastrophic earthquake and tsunami occurred on March 11, 2011, causing massive destruction over a wide area in northeastern Japan, damaging Fukushima Dai-ichi Nuclear Power Plant (FDNPP), resulting in the accidental dispersal of radionuclides.[1,2] The release of radioactive materials caused widespread contamination across Fukushima Prefecture, predominantly contaminating forested areas.[3,4] The quantity of radionuclides released and atmospheric conditions during the release have been assessed.[1,5−7] Nonetheless, there is little information on the influence of weather conditions on radionuclide deposition (i.e., during precipitation or dry weather; wet vs dry deposition) and the subsequent dynamics of radionuclides in terrestrial ecosystems, especially forests. Understanding the influence of deposition mode on resulting terrestrial radionuclide dynamics has broad implications. An enhanced understanding of how wet or dry deposition impacts movement of radionuclides in the environment will provide more accurate human and ecological risk assessments. Models of radionuclide transport and environmental accumulation after deposition are useful for predicting dispersion of other types of pollutants which ultimately accumulate in terrestrial ecosystems due to wet and dry deposition processes, such as pesticides,[8−10] heavy metals,[11−13] and numerous types of organic pollutants.[14]

Radionuclides released to the atmosphere may be deposited because of dry and wet deposition on soil and vegetation.[15−18] The first step in wet deposition via rainout is the incorporation of airborne particles and gases into cloud droplets, while the second step is delivery of the contaminated rainwater to the surface. After delivery to the surface, some fraction of deposited radionuclides is retained by the vegetation, and the rest falls and deposits on the underlying soil.[19] Other factors will influence these general steps (Table 1). Additionally, leaf and plant stand characteristics influence the initial interception and subsequent retention of atmospheric radioactive materials. Interception of radionuclides by foliage intensifies with increasing biomass per unit area.[16,20] Plant retention of radionuclides decreases with increasing rainfall intensity (wet deposition).[21]

Received: May 14, 2022
Revised: September 30, 2022
Accepted: October 4, 2022
Published: October 14, 2022

ACS Publications © 2022 American Chemical Society

Table 1. Factors that Impact Wet and Dry Deposition

factor	deposition mode	
	wet	dry
particle size <0.1 μm diameter	consisting of water-soluble material, favorable for cloud condensation nuclei	dry deposition increases with decreasing particle diameter; particle agglomeration might occur
particle size 0.1−1.0 μm	same as above	too large to be deposited quickly by Brownian diffusion and too small to be deposited quickly by inertial impaction; thus, size allows it to travel a long distance
particle size >1.0 μm	removed from atmosphere after few precipitation events; can be removed by impaction onto leaves and other obstacles	gravimetric settling, does not easily enter atmosphere
surface roughness[a]	cloud interception can occur, that is, impaction of cloud droplets at the top of tall mountains	increased surface roughness increases dry deposition
standing biomass	increased biomass increases canopy interception	increased biomass increases dry deposition

[a]The surface roughness of an area is a parameter that determines how radionuclides interact with the ground surfaces (both horizontal and inclined surfaces). The surface roughness increases with the height of the vegetation and biomass per unit area.

Dry deposition is quantified by the deposition velocity. Deposition velocity is the ratio of radionuclide deposition on land to time integrated activity concentration in air. The dry deposition velocity is a function of the particle size, chemical form of the radionuclide (i.e., reactive, and nonreactive), and wind speed.[19,22−24] Dry deposition depends on characteristics of the particles as well as the deposition surface (Table 1). Dry deposition increases in the following order: water surface < flat unvegetated land < farmland with vegetation < forests.[23,25]

The majority of the FDNPP total atmospheric deposition over land surfaces was via wet deposition.[2,7,26,27] However, the contamination in high forested southwestern regions was via dry deposition.[26,27] Higher radiocesium concentrations in vegetation, soils, and aboveground tree biomass are hypothesized to be a result of dry deposition of radiocesium.[5,28] Dry deposition of radiocesium contamination on grass, foodstuff, and other environmental materials was higher than wet deposition areas surrounding the Chornobyl Nuclear Power Plant (CNPP).[19,22,23,29] The deposition mode is important for predicting early phase radionuclide movement in the terrestrial environment, contamination levels, and uptake by trees. Models should consider wet and dry deposition pathways to better estimate radiocesium concentrations in trees.

Radiocesium deposition was greatest in forested areas of Fukushima. Radiocesium in the forested areas was expected to recycle in the ecosystem for a long period.[7,30,31] Most radiocesium was expected to be trapped by the forest canopy and gradually move to organic and mineral soil layers, similar to the CNPP accident.[15,23,32−35] However, studies demonstrated that radiocesium behavior within Fukushima forests were dependent on tree species composition,[5,36] interactions between neighboring trees,[37] spatial distribution of stems,[38] vegetation biomass,[20] and hydrological processes[39,40] that escalated the transport of particulates from plant canopies to forest floors.[7] These factors, in addition to deposition mode, introduce multiple challenges in predicting radiocesium behavior and estimating radioactivity levels in forests.[7,27,30] No studies have compared contamination measurement data to the initial mode of atmospheric deposition while considering various forest stand characteristics. Elucidating initial radiocesium dynamics in forests of different dominant species and stand densities to wet and dry deposition modes could better forecast radiocesium behavior.

We measured ambient dose rates, radiocesium concentrations, and inventories across multiple types of Fukushima Prefecture forest stands in 2011 and 2016. We also utilized radiocesium activity concentrations in various tree components (i.e., branches, leaves, and wood) from a large data set.[41] Our approach used the initial ^{137}Cs terrestrial concentrations following the Fukushima accident[42] to normalize measurement data, combined with spatial mapping of the ratio of wet deposition to the total ^{137}Cs deposition.[26] Next, the mode of ^{137}Cs deposition was estimated for each forest. This methodology allowed us to evaluate the influence of wet and dry deposition on forests of varying species and tree stand densities. Thus, we assessed conditions that may cause higher levels of ^{137}Cs deposition on forests and increased ambient dose rates. We hypothesize that contamination produced by dry deposition in dense forests caused higher ^{137}Cs concentrations in forests.

■ MATERIALS AND METHODS

Emergency Radiological Monitoring of Fukushima Forests by MAFF. The Ministry of Agriculture, Fishery and Forestry of Japan (MAFF) measured ambient radiation dose rates and activity concentrations of radiocesium in organic material and soil in 391 forest stands within Fukushima Prefecture (Figure S1) between September 16 and November 9, 2011.[43,44] Forest stands were distributed inside a 4 km interval grid within an 80 km radius of the power plant and inside a 10 km interval grid outside of the 80 km radius. At each forest stand, four organic material samples and soil cores were collected, as well as co-physiological characteristics, including stand density and the forests' dominating species. Stand density measurements were performed following the MAFF survey guidelines and procedures.[45]

Ambient dose rates were measured 1 m above the ground surface using a NaI(Tl) scintillation survey meter (TCS-172B) at each measurement site (Figure S1). A 625 cm^2 (25 × 25 cm) square frame was placed on the forest floor to indicate the sampling area (Figure S2). The organic material in the frame was collected in a plastic bag and 0−5 cm of soil was collected using a soil sampling cylinder (volume: 100 cm^3, height: 5 cm) at two locations (as far apart as possible) within the area. Sampling was repeated 20 m away toward each of the four main cardinal directions from the center (Figure S2). At each sampling point, if the outer 2 m of the area was obstructed (i.e., fallen trees, debris, and roads), the sampling site was moved to a point where sampling was possible within a 1 m perimeter. If sampling was not possible within the 1 m perimeter, then the sample was not collected.

https://doi.org/10.1021/acs.est.2c03451
Environ. Sci. Technol. 2022, 56, 15541−15551

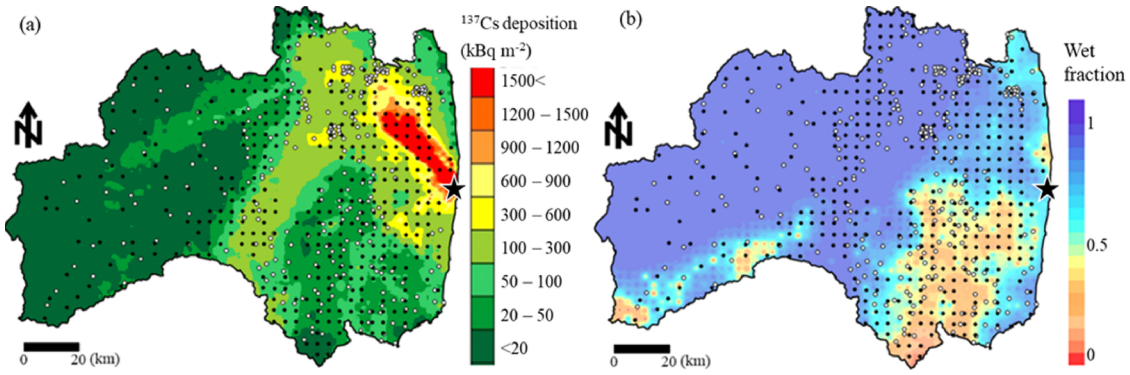

Figure 1. Locations of radiological measurement sites (organic material samples, soil samples, and ambient dose rates) at forested areas across Fukushima Prefecture. MAFF emergency measurement campaign[44] and extracted Prefectural data[41] are represented by black and white dots, respectively. Overlay spatial distribution maps include (a) reconstructed map of the Fukushima accident-derived radiocesium initial deposition[42] and (b) wet fraction ^{137}Cs deposits at the end of March 2011 based on the WSPEEDI-II system.[26] The FDNPP site is indicated by a star on both maps.

Sample Processing for Radiocesium Analysis. Organic material samples were homogenized into pieces 4 mm or less using a pestle and mortar. Organic material samples were air-dried and then dried at 70 °C for 24 h. Soil samples had stones removed and were thoroughly homogenized. Soil samples were air-dried and then dried at 105 °C for 24 h. Dried organic material and soil samples were then transferred to separate pre-weighed 100 mL containers (diameter = 50 mm; height = 62 mm; U8, Yamayu, Japan) and stored until radiocesium analysis. Derivation of ^{137}Cs deposition density (Bq m^{-2}) was calculated using mass-based measurement results (Bq kg^{-1} d.w.) and the soil bulk density based on the recorded sample area.

Radiocesium Analysis of Soil and Organic Material. The ^{134}Cs (605 and 796 keV) and ^{137}Cs (662 keV) in organic material and soil were measured using a high-purity germanium detector (HPGe; GC3018, Canberra Industries Inc., Japan, Tokyo). An efficiency calibration of the detector was performed with volume radioactivity standard gamma sources (MX033U8PP, Japan Radioisotope Association, Tokyo, Japan). Samples were counted from 1000 to 40,000 s to achieve a standard deviation <10%. Detection limits in samples were 10 Bq kg^{-1} for ^{134}Cs and ^{137}Cs.

Repeated Radiological Monitoring in 2016 by the University of Tsukuba. We visited 100 of the exact locations used by MAFF in 2011 between September and November 2016[3,43] and remeasured ambient dose rates, activity concentrations of radiocesium in organic material and soil materials, as well as contaminant densities (Figure S1). Priority was given to forests dominated by Japanese cedar (*Cryptomeria japonica*) or Japanese pine trees (*Pinus densiflora*). Precedence was given to sites with an estimated initial ^{137}Cs deposition density > 5 kBq m^{-2}. Ambient dose rate measurements (1 m above ground surface), sampling procedures, and radiocesium analyses followed the same protocols as the MAFF campaign in 2011. However, our repeated measurements collected five samples of soil and organic material to reduce the influence of Cs spatial variability on the forest floor.[46]

Extracted Measurement Data. Data published from 2011 to 2017 were used to extract a subset of 825 samples of ^{137}Cs values (in Bq kg^{-1}) in Fukushima Prefecture tree components (branch, leaves, bark, and wood).[41]

Spatial Datasets. The ratio of wet deposition to total ^{137}Cs atmospheric deposition (i.e., wet fraction) and estimated initial deposit D (kBq m^{-2}) at each forest stand site was determined using an atmospheric dispersion model[26] and the "Reconstructed initial fallout map of the Fukushima accident-derived radiocesium",[42] respectively (Figure 1). All data from both spatial data sets were transformed into continuous curved face contours using kriging 3D software SURFER 8.0.

Wet fractions from Katata et al.[26] were estimated using the Worldwide version of System for Prediction of Environmental Emergency Dose Information (WSPEEDI-II).[47] The WSPEEDI-II model was based on a refined ^{137}Cs source term combining environmental measurements of ^{137}Cs (air concentration, Bq m^{-3}) with simulations of the atmospheric dispersion using a reverse estimation method.[26] The refined ^{137}Cs source term was used to estimate the release rates of radionuclides (Bq h^{-1}) and the deposition plume. New meteorological input data and modified schemes for dry, wet, and fog-water depositions of gaseous and particulate radionuclides based on existing modeling approaches were also incorporated.

Airborne monitoring measurements were coupled with 11,000 soil samples collected from approximately 2200 different locations in Fukushima to produce distribution maps for the gamma-emitting radionuclides.[48,49] The reconstructed ^{137}Cs distribution map combined airborne surveys to further reduce measurement uncertainties.[42] Values were also adjusted for variation in the measured radioactivity associated with the influence of radioactive decay, land use types, natural weathering processes, and variation in the instrument calibration procedures.[42]

Normalization by the Deposit. Normalization included setting the same reference date for samples, and it was assumed that the release rate of ^{134}Cs and ^{137}Cs was 1:1 for ambient dose rates.[1,47] Radiological measurements and contaminant densities at all forest sites were normalized by the initial deposit D (Bq m^{-2}) and interpolated onto the same spatio-temporal frame (Figure 1) to enable comparison and consistency between sites. Normalization was performed based on Gonze et al.[37] and IAEA.[50] Normalized values of ambient dose rate in air were based on initial deposit D of ^{137}Cs at each site (per unit of ^{137}Cs ground deposition, i.e., μSv h^{-1} per kBq m^{-2}). Normalized concentrations were in m^2 kg^{-1} d.w., while inventories (i.e., inventory ratios) were unitless. The initial deposit D was subtracted from contaminant densities of organic and soil data to obtain canopy interception

https://doi.org/10.1021/acs.est.2c03451
Environ. Sci. Technol. 2022, 56, 15541−15551

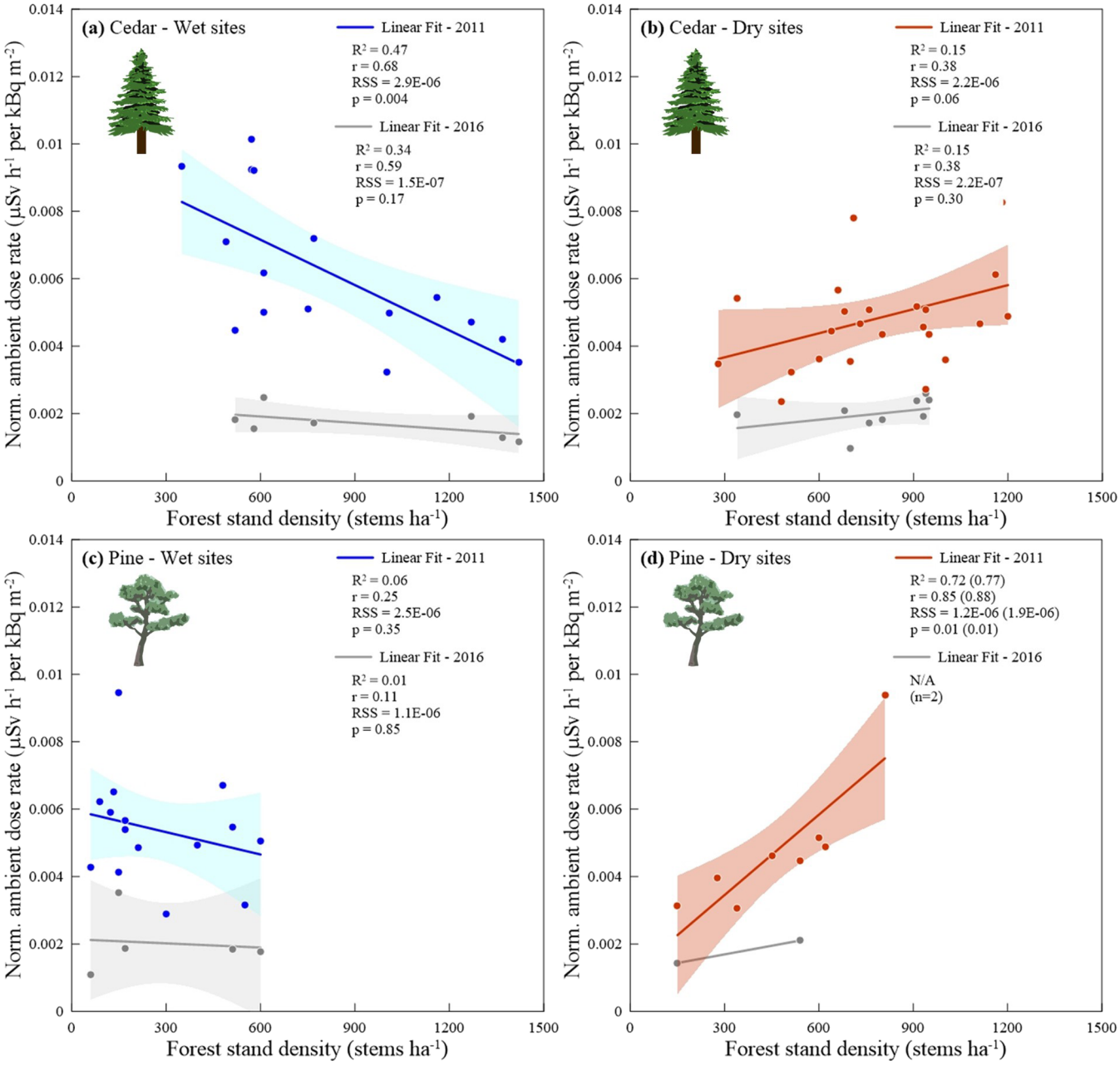

Figure 2. Normalized ambient dose measurements (μSv h^{-1} per kBq m^{-2}) as a function of forest stand densities (trees ha^{-1}) for wet sites (blue) and dry sites (red). (a) Measurements at Japanese cedar (*Cryptomeria japonica*) forest stands in 2011 and 2016, in which the original ^{137}Cs deposition following release was primarily wet deposition or (b) dry deposition. (c) Measurements at Japanese red pine (*Pinus densiflora*) forest stands in 2011 and 2016, in which the original ^{137}Cs deposition following release was primarily wet deposition or (d) dry deposition. Regression lines are represented as solid lines, and the shading indicates the 95% confidence interval of the ambient dose rate. Solid gray lines indicate data from 2016. Gray shading indicates the 95% confidence interval of ambient dose rates in 2016. Regression statistics are provided in (a−d). In (d), one data point with a large residual was removed and subsequent statistics are provided in parentheses. No clear trends or statistical significances were observed for 2016.

estimates. The relationship between the time dependence of gamma-dose rate and the ^{137}Cs levels per unit area is of nonlinear nature due to the different decay rates of ^{134}Cs and ^{137}Cs. However, assuming a release rate of 1:1, the composition of the radionuclides contributing to ambient dose rates would not influence interpretations of results, and initial ^{137}Cs deposition could be used to normalize the measured ambient dose.

Data Processing and Analysis of Wet and Dry Deposited ^{137}Cs. The original analysis was done by plotting radiological measurement data as a function of the wet fraction. Once we identified that the trend between treatments was clearer, the dataset was classified into two groups according to the dominant deposition mode. Sites with less than 50% wet deposition compared to the total ^{137}Cs atmospheric deposition were defined as "dry sites" (i.e., sites contaminated primarily by dry depositional processes). Sites with greater than 90% wet deposition were defined as "wet sites" (i.e., sites contaminated primarily by wet depositional processes). Dry deposition was predominant in studies with higher ^{137}Cs concentrations in

https://doi.org/10.1021/acs.est.2c03451
Environ. Sci. Technol. 2022, 56, 15541−15551

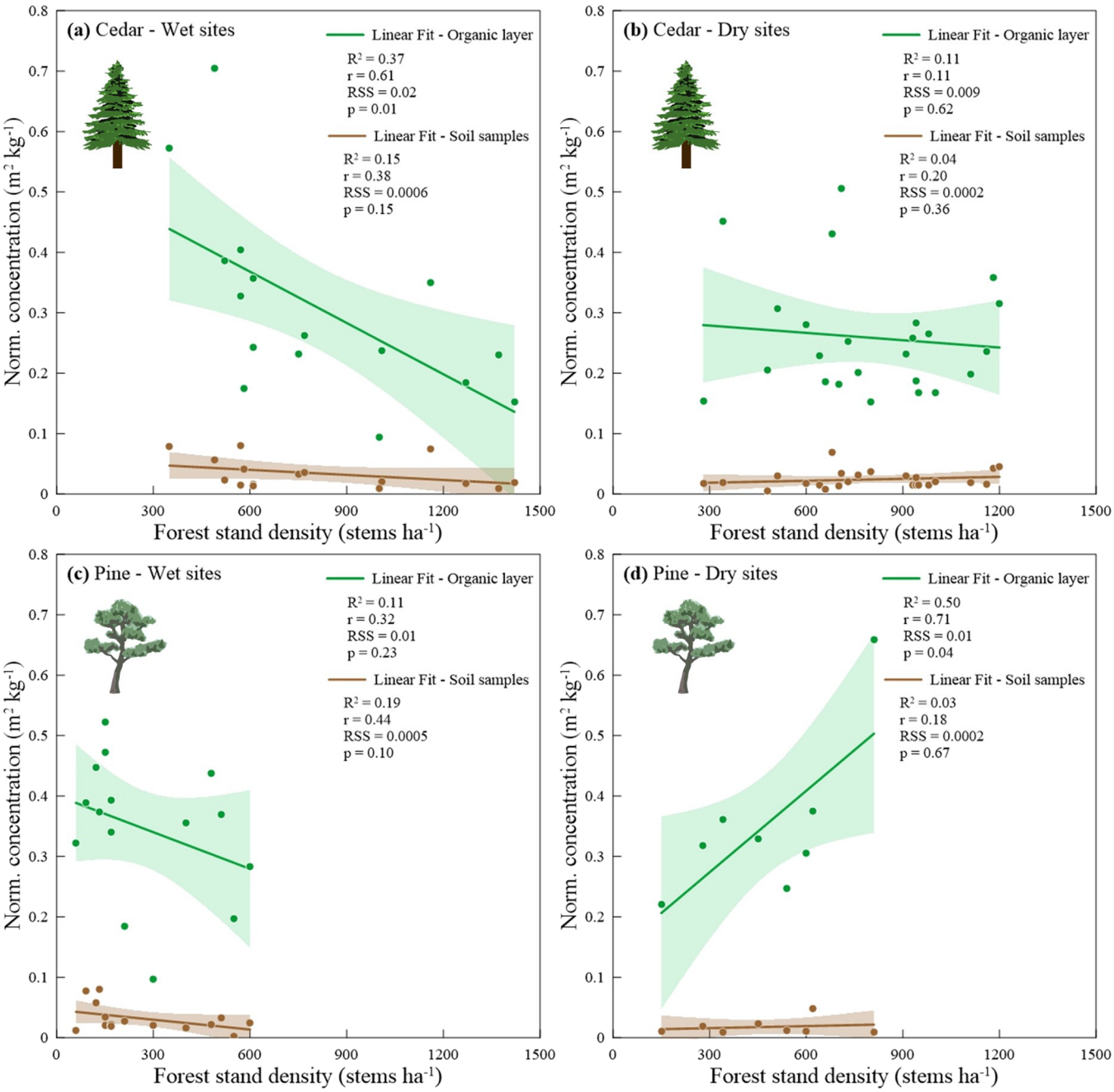

Figure 3. Normalized activity concentrations ($m^2\ kg^{-1}$) in the organic layer (green) and soil samples (brown) as a function of forest stand densities for wet and dry sites. Regression lines are represented as solid lines; shading indicates the 95% confidence interval of activity concentrations. (a) Sampling at Japanese cedar forest stands in 2011 in which the original ^{137}Cs deposition following release was wet deposition or (b) dry deposition. (c) Sampling at Japanese red pine forest stands in 2011 in which the original ^{137}Cs deposition following release was primarily during precipitation or (d) deposited as dry particles. In 2016, no trends were observed for (a−d), please see Figure S4.

vegetation, forest floor materials, or soils.[5,28] Forest stands that had either Japanese cedar (*Cryptomeria japonica*) or Japanese pine trees (*Pinus densiflora*) as the dominate species (or > 75% of tree stems) were selected for study. Forest stands of other species had too few sites to assess and were excluded.

Limitations and Uncertainties. Interception of wet and dry deposition by vegetation is important during and shortly after the release of radionuclides.[15,51] Radionuclides are transferred from vegetative surfaces by wash-off from precipitation, loss of leaves, abrasion by wind, and other factors after deposition ceases. Our analyses used emergency sampling data initiated some six months postaccident (between 16 September and 9 November 2011); immediate sampling was not possible because the highly contaminated forests were too hazardous to workers. An estimated 50−60% of radionuclides deposited in cedar and pine forests remained in tree crowns during the 2011 sampling period[28,36] and had not been lost through transfer processes before initial sample collection. The contamination measured in autumn was thought to reflect general contamination patterns immediately postdeposition.

Reverse modeling used to estimate wet to total deposition of ^{137}Cs is a study limitation.[26] The small number of publicly

https://doi.org/10.1021/acs.est.2c03451
Environ. Sci. Technol. 2022, 56, 15541−15551

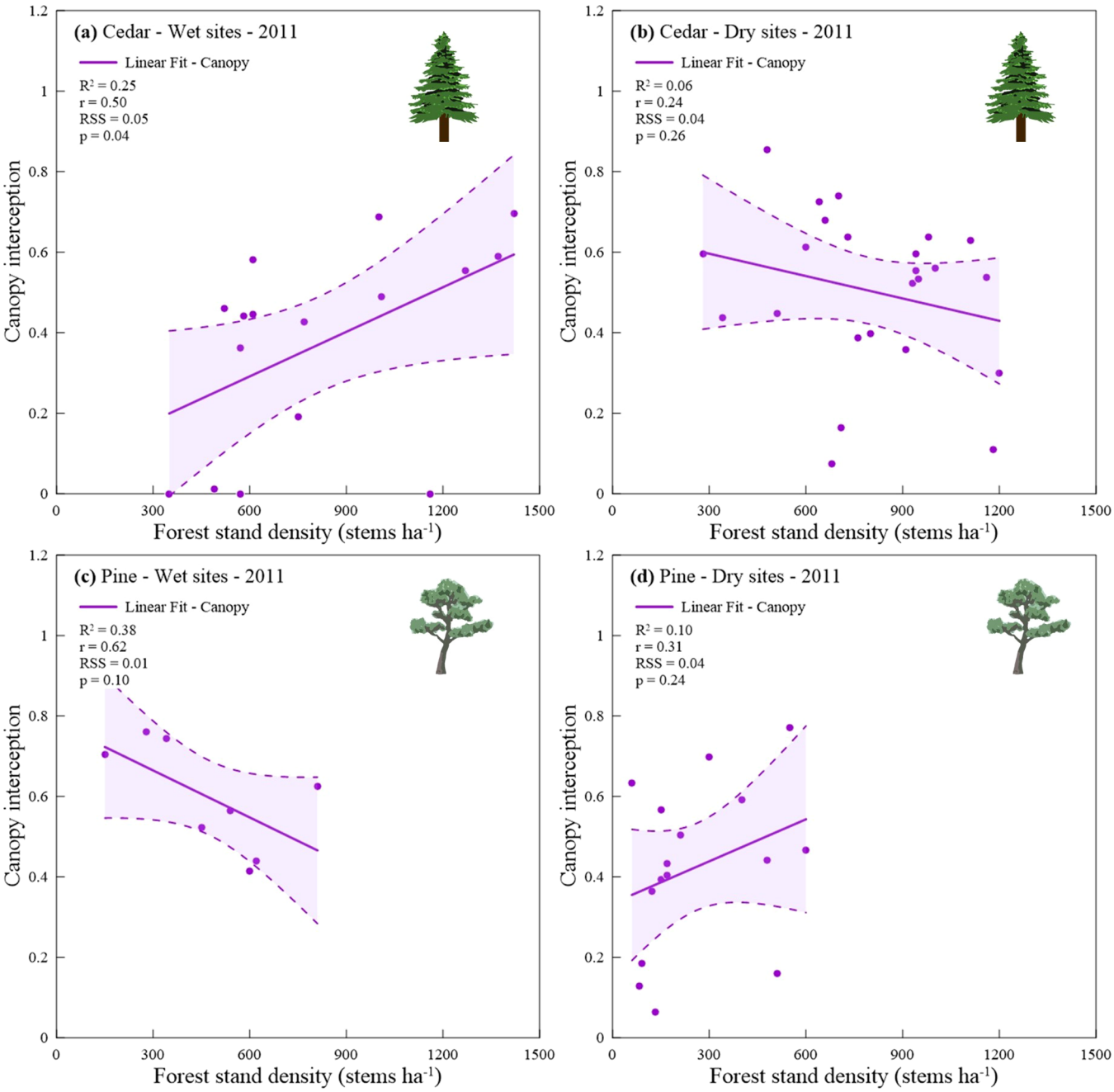

Figure 4. Canopy interception (purple) as a function of forest stand densities for wet and dry sites. Regression lines are represented as solid lines, and the shading indicates the 95% confidence interval of canopy interception. (a) Sampling at Japanese cedar forest stands in 2011, in which original ^{137}Cs deposition was primarily during precipitation or (b) dry deposition. (c) Sampling at Japanese pine forest stands in 2011, in which the original ^{137}Cs deposition following release was primarily during precipitation or (d) dry deposition.

released environmental measurements and the estimation of errors described in Winiarek et al.[52] add to modeling uncertainty. However, Katata et al.[26] has incorporated a vast amount of released environmental measurement data including information for dry, wet, and fog−water depositions. Reasonable results are expected for large spatial forest sites in this study, with increased uncertainty for smaller sites. We considered such estimation uncertainties in determination of the dominant deposition mode by the atmospheric transport model and the areas of extreme difference in deposition mode were selected (e.g., >90% for the wet-dominated area). However, to obtain a reasonable number of data for dry-dominated areas, a wider range of <50% wet deposition was classified as dry-dominated. Additionally, dry site classification (areas that received less than 50% wet deposition) was based on only a few studies.[5,7,28] Future studies will need to assess classifications as data become more available.

RESULTS AND DISCUSSION

Dry vs Wet Deposited ^{137}Cs in Forest Stands. Wet deposition was dominant in the western part of Fukushima Prefecture forest sites and northwest of FDNPP (Figure 1). Dry deposition dominated southwestern forest sites with wet deposition generally less than 50%. The deposition mode was

https://doi.org/10.1021/acs.est.2c03451
Environ. Sci. Technol. 2022, 56, 15541−15551

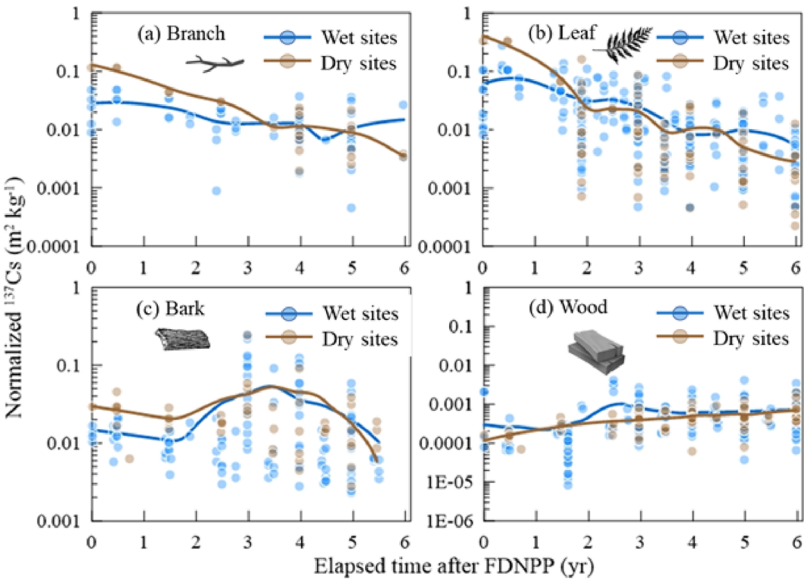

Figure 5. ^{137}Cs concentrations in elapsed above ground biomass compartments, (a) branch, (b) leaf, (c) bark, and (d) wood. Samples from 2011−2018 were obtained from Hashimoto et al.[41] The ^{137}Cs concentration levels were normalized using estimated initial deposit D (kBq m^{-2}) at each sampling site obtained from the "Reconstructed initial fallout map of the Fukushima accident-derived radiocesium."[42] Samples were classified as wet sites (blue) or dry sites (brown) based on the site's wet fraction estimate by of the atmospheric dispersion model.[11] Following this approach, 825 samples were used (602 wet (blue lines) and 223 samples dry (brown lines)). (a−d) Nonparametric local regression line of best fit was used for fitting smooth curves to empirical data.

correlated with normalized ambient dose measurements (1 m above the forest floor) among Japanese cedar and Japanese pine trees when tree stand density was considered (Figure 2). Additionally, the decline in normalized ambient dose rates in forest from 2011 to 2016 was largely due to ^{134}Cs decay.

For predominantly wet deposition of ^{137}Cs, the normalized ambient dose rate in cedar forest (μSv h^{-1} per kBq m^{-2}) declined with increasing stand density (Figure 2). In cedar forests with predominantly dry ^{137}Cs deposition, the dose rates increased with increasing stand density (Figure 2).

A greater number of stems in dense evergreen forests may cause a shielding effect that results in reduced dose rates. In general, interception of wet deposited radionuclides increases with increasing stand density and thus less activity reaches the ground, resulting in a decrease of ambient dose rates (i.e., decrease because the radiation is attenuated by the dense forest canopy). Total dry deposition increases with increasing stand density because of the larger filtering capacity of well-developed forest canopies[33] causing an increase of the normalized ambient dose rate. Shielding effects by the forest canopy were less important for dry deposition sites. The shielding effect observed needs to be investigated in deciduous forests as leaves had not emerged at the time of deposition. Greater ^{137}Cs contamination occurred in evergreen forest canopies, compared with deciduous trees,[39,53] which may have caused radiation attenuation observed.

There is no clear ambient dose rate trend for wet deposition in pine tree forests (Figure 2). An increase of the dose rate with increasing stand density was observed for dry deposition; however, a precise estimate will require a larger sample size. Additionally, pine tree results may be influenced by one data point with a large residual. A statistical increase in dose with increasing stand density ($R^2 = 0.77$; $p = 0.01$) is observed when the large residual data point is removed. Generally, Japanese red pine shed leaves in early autumn, while the Japanese cedar sheds in late autumn and winter.[5,53] The increase in ambient dose rates with increasing stem density observed in pine forests may be due to the early shedding of potentially contaminated leaves and needles (Figure 2).

Canopy morphology differences (e.g., stem density, leaf area index (LAI), and the canopy height) could impact contamination patterns.[54,55] In 2011 and 2012, the contribution of forest canopy radiocesium to ambient dose rates at 1 m height varied depending on forest stand characteristics.[56] Radiocesium retained in the cedar forest canopy contributed more to ambient dose rates than other canopies.[56] Our modeled decrease in the dose rate in dense forests is supported by measurements of Komatsu et al.,[5] Malins et al.,[56] and Kato et al.[57]

Normalized activity concentrations in the organic material of cedar forests also decreased with increasing forest density for wet deposition (Figure 3a), but soil did not. The ^{137}Cs concentrations in forest floor organic matter and soil were strongly correlated to ambient dose measurements ($R^2 = 0.91$, Figure S3). Thus, the organic layer contributed more to the measured ambient dose rate than the topsoil layer in 2011. No trends for the initial deposition mode were observed in 2016, indicating both species of forest stands entered a similar phase of ^{137}Cs redistribution (Figure S4). The transport of radiocesium to forest floors and cycling processes[39,40,58] will eventually occur in all forests regardless of species and deposition mode.

Radiocesium Contamination in Forest Floors and Migration to Soil Layers. An XLSX supplemental file contains ^{137}Cs activity concentrations (Bq kg^{-1}) in organic materials, soil samples, and surface contaminant densities (Bq m^{-2}), for the Fukushima forest sites (Figure S5). Normalized radiocesium activity concentrations and contaminant densities were higher in organic material compared to the top soil for the first 200 days.[7,36,48,57] Our models indicated that an average of 60% of deposited ^{137}Cs remained in the organic material (20%) and upper soil layers (40%) six months after

https://doi.org/10.1021/acs.est.2c03451
Environ. Sci. Technol. 2022, 56, 15541−15551

the accident (all 390 sites), agreeing well with reports that 50−70% of contaminants retained in these layers.[7,37] Five years postaccident, ^{137}Cs levels declined approximately 24% in forest floor samples (11% due to radioactive decay and 13% redistribution in the environment) with most ^{137}Cs in upper soil layers (64%) rather than the organic material (6%). Trends in the rate of ^{137}Cs decline in organic material differed between forest sites. The activity concentration decrease was greater for pine than for cedar forests.

Atmospheric deposition mode and stand density influenced contaminant densities on forest floors (Figure S6) and canopy interception (Figure 4). Dry deposition resulted in increased canopy interception for both cedar and pine forests (e.g., 50 and 60% for cedar and pine, respectively) compared to wet depositional processes (35 and 43% for cedar and pine, respectively). Total deposition intercepted by canopies during precipitation was lower in cedar forests with low stem densities, and the canopy interception of radiocesium increased with increasing biomass per unit area. Leaf area index (LAI), not stem density, could have a more direct effect on radiocesium interception. Generally, the higher the stand density, the greater the leaf cover, and the leaf area represents the main interface between atmosphere and plant canopies.[17] A greater LAI is known to cause greater interception of pollutants.[17]

Factors Controlling Early Radiocesium Redistribution and Uptake by Trees. Dry deposition resulted in higher ^{137}Cs concentrations in above-ground biomass compartments of trees (i.e., bark, leaves, and branches), but not the wood compartment (p = 0.32) (Figures 5 and S7). The lack of hydrological processes to transport ^{137}Cs to forest floors (or higher canopy interception) may be the reason dry deposition resulted in increased concentrations in tree compartments.[16,23,27] Bioaccumulation of ^{137}Cs by inner tree compartments was not influenced by deposition mode. Rather, an extended period of time was needed for the radioactivity to enter into wood by root uptake from soil, followed by translocation throughout the tree.[59−61] However, only a few dry deposition data points were available for 2011, so caution should be used in interpretation of dry deposition results. Deposition mode (wet or dry) is an important consideration for ^{137}Cs accumulation in the environment, as supported by other studies of Fukushima[5,7,28] and the CNPP accident.[19,22,29]

Dry deposition is dependent on the particle size.[16,23] Large amounts of volatile ^{137}Cs were emitted from FDNPP and attached to ambient aerosol in the size range 0.1−2 μm diameter (small dry deposition velocities).[62,63] ^{137}Cs particles with a diameter between 0.1 and 1 μm remain airborne for long distances and do not deposit at high rates close to the release (Table 1). Larger ^{137}Cs particles (>1 μm) likely deposited nearby the release site via dry deposition due to gravitational settling and inertial impaction, as well as some interception.[24,27] Some large particles may be subject to more efficient wet deposition because the large particles may be activated as condensation nuclei before smaller particles,[64] if the particles are hygroscopic. Smaller particles (0.1−1 μm) are more likely to be deposited at increased distances from FDNPP (Table 1). Additionally, the particle size affects subsequent adsorption of ^{137}Cs by soils[65] and therefore translocation to above-ground biomass compartments of trees. Many areas classified as dry sites in this study received some precipitation. Precipitation, such as rainfall, produces moisture on plant canopies and vegetation, which may have greatly enhanced dry deposition of particles by reducing particle "bounce".[16] Thus, the wetting of plant surfaces prior to dry deposition may increase or decrease the rate of particle resuspension, depending on the particle size and influence contamination of vegetation.[15,66]

The CNPP and FDNPP accidents demonstrated the complexity of radioactive atmospheric deposit redistribution in forests[5,7,23,37] and the multiple physical mechanisms influencing the interaction of various factors during early phases (<200 days).[5,57,67] ^{137}Cs particles captured by canopies were translocated to forest floors by rainwater and leaf-fall, then recirculated within the ecosystem in each accident. The translocation of ^{137}Cs to cedar forest floors where wet deposition occurred was lower than that of other cedar stands with lower stand densities. The reduced rate at which contaminants are removed from the canopy could be attributed to greater needle biomass influencing initial fallout interception.[53] Forests with low stem densities were influenced by washout (entrainment of particles by rainfall) that accelerated ^{137}Cs transport to forest floors causing increased dose rates, soil activity concentrations, and ground deposition. In a dry deposition-dominated area, dense forests capture more atmospheric ^{137}Cs because of the efficient filtering capacity of the dense canopy, causing more contamination of above-ground biomass compartments of trees.

Significance of Results. Deposition mode (wet or dry) influences the resulting radionuclide dynamics in a forest. The interaction of the deposition mode and the forest stand characteristics control the early stages of ^{137}Cs cycling processes and the fraction of radiocesium depositing directly onto the forest floor. The initial retention of radiocesium increases with the stem density. Dry deposition of ^{137}Cs was retained in the forest canopy longer compared to the wet deposition of ^{137}Cs. However, the robustness of these conclusions is limited by the small number of dry sites, uncertainties associated with modeling, and modes of deposition. Limited data are available to validate estimations of the ratio of wet deposition to total ^{137}Cs atmospheric deposition by atmospheric transport models. The results of this study indicate the possibility that field data in Fukushima forests may allow the validation of the model output.

No differences in ^{137}Cs distribution due to dry and wet deposition were observed after five years. The ratio of wet and dry deposition appears to only influence the interception (initial retention of radionuclides) by the forest canopy. The transfer of ^{137}Cs from the canopy to the forest floor and radiocesium cycling will eventually dominate radiocesium behavior. Generalization to all forests may not be possible due to other site-specific factors that may influence the initial ^{137}Cs distribution because this study was limited to evergreen forests. For example, the initial retention of ^{137}Cs and initial activity levels in the above ground parts of deciduous forests might also be influenced by the deposition mode as their canopies generally have greater biomass per unit area than evergreen forests depending on the season. Nevertheless, the deposition mode is an important factor in determining the extent of the above ground forest contamination immediately after a release. Decisions on early decontamination efforts and decisions on occupation of forests can be impacted by the deposition mode, and further analyses will aid our understanding of the long-term dynamics of Cs in forest ecosystems.

https://doi.org/10.1021/acs.est.2c03451
Environ. Sci. Technol. 2022, 56, 15541−15551

■ ASSOCIATED CONTENT

Supporting Information

The Supporting Information is available free of charge at https://pubs.acs.org/doi/10.1021/acs.est.2c03451.

Locations for measurements of ambient dose rates and sampling of soils and organic material; additional experimental details, materials, and methods, including photographs of experimental setup; plotted ^{137}Cs concentrations of soils and organic material; and box plot analysis of ^{137}Cs in above biomass compartments (PDF)

Field measurement data from 2011 and 2016 surveys; data include ambient dose rates (1 m above the surface); ^{134}Cs and ^{137}Cs in organic materials and 0−5 cm soil samples; ^{137}Cs contaminant densities; and forest measurements and observations (XLSX)

■ AUTHOR INFORMATION

Corresponding Authors

Donovan Anderson − *Institute of Radiation Emergency Medicine, Hirosaki University, Hirosaki City 036-8564, Japan; Center for Research in Isotopes and Environmental Dynamics, University of Tsukuba, Tsukuba City 305-8577, Japan*; orcid.org/0000-0001-6716-4059; Email: ande4163@hirosaki-u.ac.jp

Yuichi Onda − *Center for Research in Isotopes and Environmental Dynamics, University of Tsukuba, Tsukuba City 305-8577, Japan*; Email: onda@geoenv.tsukuba.ac.jp

Author

Hiroaki Kato − *Center for Research in Isotopes and Environmental Dynamics, University of Tsukuba, Tsukuba City 305-8577, Japan*

Complete contact information is available at: https://pubs.acs.org/10.1021/acs.est.2c03451

Notes

The authors declare no competing financial interest.

■ ACKNOWLEDGMENTS

We would like to acknowledge the Ministry of Agriculture, Fishery and Forestry of Japan for sample collection. This work was supported by AMORAD project by IRSN [Grant Number ANR-11-RSNR-0002] and Japan Atomic Energy Agency [FY2015−2021]. Any opinions, findings, conclusions, or recommendations expressed in this material are those of the author(s) and do not necessarily reflect the views of the IRSN or JAEA. The authors declare no conflict of interest.

■ REFERENCES

(1) Chino, M.; Nakayama, H.; Nagai, H.; Terada, H.; Katata, G.; Yamazawa, H. Preliminary Estimation of Release Amounts of ^{131}I and ^{137}Cs Accidentally Discharged from the Fukushima Daiichi Nuclear Power Plant into the Atmosphere. *J. Nucl. Sci. Technol.* **2011**, *48*, 1129−1134.

(2) Morino, Y.; Ohara, T.; Watanabe, M.; Hayashi, S.; Nishizawa, M. Episode Analysis of Deposition of Radiocesium from the Fukushima Daiichi Nuclear Power Plant Accident. *Environ. Sci. Technol.* **2013**, *47*, 2314−2322.

(3) Kato, H.; Onda, Y.; Yamaguchi, T. Temporal Changes of the Ambient Dose Rate in the Forest Environments of Fukushima Prefecture Following the Fukushima Reactor Accident. *J. Environ. Radioact.* **2018**, *193-194*, 20−26.

(4) Hashimoto, S.; Ugawa, S.; Nanko, K.; Shichi, K. The Total Amounts of Radioactively Contaminated Materials in Forests in Fukushima, Japan. *Sci. Rep.* **2012**, *2*, 416.

(5) Komatsu, M.; Kaneko, S.; Ohashi, S.; Kuroda, K.; Sano, T.; Ikeda, S.; Saito, S.; Kiyono, Y.; Tonosaki, M.; Miura, S.; Akama, A.; Kajimoto, T.; Takahashi, M. Characteristics of Initial Deposition and Behavior of Radiocesium in Forest Ecosystems of Different Locations and Species Affected by the Fukushima Daiichi Nuclear Power Plant Accident. *J. Environ. Radioact.* **2016**, *161*, 2−10.

(6) Saito, K.; Mikami, S.; Andoh, M.; Matsuda, N.; Kinase, S.; Tsuda, S.; Yoshida, T.; Sato, T.; Seki, A.; Yamamoto, H.; Sanada, Y.; Wainwright-Murakami, H.; Takemiya, H. Summary of Temporal Changes in Air Dose Rates and Radionuclide Deposition Densities in the 80 Km Zone over Five Years after the Fukushima Nuclear Power Plant Accident. *J. Environ. Radioact.* **2019**, *210*, No. 105878.

(7) Onda, Y.; Taniguchi, K.; Yoshimura, K.; Kato, H.; Takahashi, J.; Wakiyama, Y.; Coppin, F.; Smith, H. Radionuclides from the Fukushima Daiichi Nuclear Power Plant in Terrestrial Systems. *Nat. Rev. Earth Environ.* **2020**, *1*, 644−660.

(8) Daly, G. L.; Lei, Y. D.; Teixeira, C.; Muir, D. C. G.; Wania, F. Pesticides in Western Canadian Mountain Air and Soil. *Environ. Sci. Technol.* **2007**, *41*, 6020−6025.

(9) Dubus, I. G.; Brown, C. D.; Beulke, S. Sources of Uncertainty in Pesticide Fate Modelling. *Sci. Total Environ.* **2003**, *317*, 53−72.

(10) Chen, W.; Wiepke, T.; Snyder, N. In Situ Measurements of Soil Hydrology in a Field Dissipation Study: Implications for Understanding Pesticide Residue Movement. In *Terrestrial Field Dissipation Studies*; ACS Publications, 2002; pp. 117−136.

(11) Morrissey, C. A.; Albert, C. A.; Dods, P. L.; Cullen, W. R.; Lai, V. W. M.; Elliott, J. E. Arsenic Accumulation in Bark Beetles and Forest Birds Occupying Mountain Pine Beetle Infested Stands Treated with Monosodium Methanearsonate. *Environ. Sci. Technol.* **2007**, *41*, 1494−1500.

(12) Zheng, X.; Guo, X.; Zhao, W.; Shu, T.; Xin, Y.; Yan, X.; Xiong, Q.; Chen, F.; Lv, M. Spatial Variation and Provenance of Atmospheric Trace Elemental Deposition in Beijing. *Atmos. Pollut. Res.* **2016**, *7*, 260−267.

(13) Taylor, P. D.; Ramsey, M. H.; Potts, P. J. Spatial Contaminant Heterogeneity: Quantification with Scale of Measurement at Contrasting Sites. *J. Environ. Monit.* **2005**, *7*, 1364−1370.

(14) Lin, T.; Han, Y.; Wu, Z.; Hu, L.; Rose, N. L.; Guo, Z. Deposition Records of Persistent Organic Pollutants and Black Carbon in Dated Sediment Cores from China Marginal Seas : Implications for Terrestrial Sources and Transport Processes. *Mar. Pollut. Bull.* **2022**, *181*, No. 113874.

(15) Anspaugh, L. R.; Simon, S. L.; Gordeev, K. I.; Likhtarev, I. A.; Maxwell, R. M.; Shinkarev, S. M. Movement of Radionuclides in Terrestrial Ecosystems by Physical Processes. *Health Phys.* **2002**, *82*, 669−679.

(16) Kinnersley, R. P.; Goddard, A. J. H.; Minski, M. J.; Shaw, G. Interception of Caesium-Contaminated Rain by Vegetation. *Atmos. Environ.* **1997**, *31*, 1137−1145.

(17) Pröhl, G. Interception of Dry and Wet Deposited Radionuclides by Vegetation. *J. Environ. Radioact.* **2009**, *100*, 675−682.

(18) Owen Hoffman, F.; Thiessen, K. M.; Frank, M. L.; Gordon Blaylock, B. Quantification of the Interception and Initial Retention of Radioactive Contaminants Deposited on Pasture Grass by Simulated Rain. *Atmos. Environ. A Gen. Top.* **1992**, *26*, 3313−3321.

(19) Kinnersley, R. P.; Scott, L. K. Aerial Contamination of Fruit through Wet Deposition and Particulate Dry Deposition. *J. Environ. Radioact.* **2001**, *52*, 191−213.

(20) Gonze, M. A.; Sy, M. M. Interception of Wet Deposited Atmospheric Pollutants by Herbaceous Vegetation: Data Review and Modelling. *Sci. Total Environ.* **2016**, *565*, 49−67.

(21) Owen Hoffman, F.; Thiessen, K. M.; Rael, R. M. Comparison of Interception and Initial Retention of Wet-Deposited Contaminants on Leaves of Different Vegetation Types. *Atmos. Environ.* **1995**, *29*, 1771−1775.

(22) Clark, M. J.; Smith, F. B. Wet and Dry Deposition of Chernobyl Releases. *Nature* **1988**, *332*, 245−249.
(23) Bunzl, K.; Schimmack, W.; Kreutzer, K.; Schierl, R. Interception and Retention of Chernobyl-Derived ^{134}Cs, ^{137}Cs and ^{106}Ru in a Spruce Stand. *Sci. Total Environ.* **1989**, *78*, 77−87.
(24) Petroff, A.; Zhang, L. Development and Validation of a Size-Resolved Particle Dry Deposition Scheme for Application in Aerosol Transport Models. *Geosci. Model Dev.* **2010**, *3*, 753−769.
(25) IAEA. *Handbook of Parameter Values for the Prediction of Radionuclide Transfer in Terrestrial and Freshwater Environments*; Technical Reports Series No. 472 ; International Atomic Energy Agency: Vienna, Austria, 2010.
(26) Katata, G.; Chino, M.; Kobayashi, T.; Terada, H.; Ota, M.; Nagai, H.; Kajino, M.; Draxler, R.; Hort, M. C.; Malo, A.; Torii, T.; Sanada, Y. Detailed Source Term Estimation of the Atmospheric Release for the Fukushima Daiichi Nuclear Power Station Accident by Coupling Simulations of an Atmospheric Dispersion Model with an Improved Deposition Scheme and Oceanic Dispersion Model. *Atmos. Chem. Phys.* **2015**, *15*, 1029−1070.
(27) Gonze, M. A.; Renaud, P.; Korsakissok, I.; Kato, H.; Hinton, T. G.; Mourlon, C.; Simon-Cornu, M. Assessment of Dry and Wet Atmospheric Deposits of Radioactive Aerosols: Application to Fukushima Radiocaesium Fallout. *Environ. Sci. Technol.* **2014**, *48*, 11268−11276.
(28) Onda, Y.; Sweeck, L.; Shinano, T.; Dercon, G.; Yi, A. L. Z.; Kato, H. Soil and Vegetation Sampling during the Early Stage of Fukushima Daiichi Nuclear Power Plant Accident and the Implication for the Emergency Preparedness for Agricultural Systems. *J. Environ. Radioact.* **2020**, *223-224*, No. 106373.
(29) Hötzl, H.; Rosner, G.; Winkler, R. Long-Term Behaviour of Chernobyl Fallout in Air and Precipitation. *J. Environ. Radioact.* **1989**, *10*, 157−171.
(30) Hashimoto, S.; Ugawa, S.; Nanko, K.; Shichi, K. The Total Amounts of Radioactively Contaminated Materials in Forests in Fukushima. *Japan. Sci. Rep.* **2012**, *2*, 1−5.
(31) Yoschenko, V.; Nanba, K.; Ohkubo, T.; Kato, H. Behavior of Fukushima-Derived Radiocesium in Forest Ecosystems. In *Behavior of Radionuclides in the Environment III*; Springer Singapore: Singapore, 2022; pp. 427−462.
(32) Tikhomirov, F. A.; Shcheglov, A. I. Main Investigation Results on the Forest Radioecology in the Kyshtym and Chernobyl Accident Zones. *Sci. Total Environ.* **1994**, *157*, 45−57.
(33) Ronneau, C.; Cara, J.; Apers, D. The Deposition of Radionuclides from Chernobyl to a Forest in Belgium. *Atmos. Environ.* **1967**, *21*, 1467−1468.
(34) Nygren, P.; Hari, P.; Raunemaa, T.; Kulmala, M.; Luokkanen, S.; Holmberg, M.; Nikinmaa, E. Behaviour of 137 Cs from Chernobyl Fallout in a Scots Pine Canopy in Southern Finland. *Can. J. For. Res.* **1994**, *24*, 1210−1215.
(35) Tobler, L.; Bajo, S.; Wyttenbach, A. Deposition of 134,137Cs from Chernobyl Fallout on Norway Spruce and Forest Soil and Its Incorporation into Spruce Twigs. *J. Environ. Radioact.* **1988**, *6*, 225−245.
(36) Kato, H.; Onda, Y.; Hisadome, K.; Loffredo, N.; Kawamori, A. Temporal Changes in Radiocesium Deposition in Various Forest Stands Following the Fukushima Dai-Ichi Nuclear Power Plant Accident. *J. Environ. Radioact.* **2017**, *166*, 449−457.
(37) Gonze, M. A.; Calmon, P.; Hurtevent, P.; Coppin, F. Meta-Analysis of Radiocesium Contamination Data in Japanese Cedar and Cypress Forests over the Period 2011−2017. *Sci. Total Environ.* **2021**, *750*, No. 142311.
(38) Imamura, N.; Levia, D. F.; Toriyama, J.; Kobayashi, M.; Nanko, K. Stemflow-Induced Spatial Heterogeneity of Radiocesium Concentrations and Stocks in the Soil of a Broadleaved Deciduous Forest. *Sci. Total Environ.* **2017**, *599-600*, 1013−1021.
(39) Endo, I.; Ohte, N.; Iseda, K.; Tanoi, K.; Hirose, A.; Kobayashi, N. I.; Murakami, M.; Tokuchi, N.; Ohashi, M. Estimation of Radioactive 137-Cesium Transportation by Litterfall, Stemflow and Throughfall in the Forests of Fukushima. *J. Environ. Radioact.* **2015**, *149*, 176−185.
(40) Saidin, Z. H.; Levia, D. F.; Kato, H.; Kurihara, M.; Hudson, J. E.; Nanko, K.; Onda, Y. Vertical Distribution and Transport of Radiocesium via Branchflow and Stemflow through the Canopy of Cedar and Oak Stands in the Aftermath of the Fukushima Dai-Ichi Nuclear Power Plant Accident. *Sci. Total Environ.* **2022**, *818*, No. 151698.
(41) Hashimoto, S.; Imamura, N.; Kawanishi, A.; Komatsu, M.; Ohashi, S.; Nishina, K.; Kaneko, S.; Shaw, G.; Thiry, Y. A Dataset of ^{137}Cs Activity Concentration and Inventory in Forests Contaminated by the Fukushima Accident. *Sci. Data* **2020**, *7*, 1−5.
(42) Kato, H.; Onda, Y. Determining the Initial Fukushima Reactor Accident-Derived Cesium-137 Fallout in Forested Areas of Municipalities in Fukushima Prefecture. *J. For. Res.* **2018**, *23*, 73−84.
(43) Ministry of Agriculture Forestry and Fisheries of Japan (MAFF). Monitoring results of ambient dose rate in forest of Fukushima Prefecture. In Japanese. https://www.rinya.maff.go.jp/j/kouhou/jisin/attach/pdf/H27izen-15.pdf (accessed 2022-03-15).
(44) Ministry of Agriculture Forestry and Fisheries of Japan (MAFF). Annual report on forest and Forestry in Japan, Fiscal year, 2011. https://www.maff.go.jp/e/data/publish/attach/pdf/index-27.pdf (accessed 2022-03-15).
(45) Ministry of Agriculture Forestry and Fisheries of Japan (MAFF). Basic survey on forest ecosystem diversity. In Japanese. https://www.rinya.maff.go.jp/j/keikaku/tayouseichousa/ (accessed 2022-03-15).
(46) Onda, Y.; Kato, H.; Hoshi, M.; Takahashi, Y.; Nguyen, M. L. Soil Sampling and Analytical Strategies for Mapping Fallout in Nuclear Emergencies Based on the Fukushima Dai-ichi Nuclear Power Plant Accident. *J. Environ. Radioact.* **2015**, *139*, 300−307.
(47) Terada, H.; Katata, G.; Chino, M.; Nagai, H. Atmospheric Discharge and Dispersion of Radionuclides during the Fukushima Dai-ichi Nuclear Power Plant Accident. Part II: Verification of the Source Term and Analysis of Regional-Scale Atmospheric Dispersion. *J. Environ. Radioact.* **2012**, *112*, 141−154.
(48) Mikami, S.; Maeyama, T.; Hoshide, Y.; Sakamoto, R.; Sato, S.; Okuda, N.; Demongeot, S.; Gurriaran, R.; Uwamino, Y.; Kato, H.; Fujiwara, M.; Sato, T.; Takemiya, H.; Saito, K. Spatial Distributions of Radionuclides Deposited onto Ground Soil around the Fukushima Dai-ichi Nuclear Power Plant and Their Temporal Change until December 2012. *J. Environ. Radioact.* **2015**, *139*, 320−343.
(49) Saito, K.; Tanihata, I.; Fujiwara, M.; Saito, T.; Shimoura, S.; Otsuka, T.; Onda, Y.; Hoshi, M.; Ikeuchi, Y.; Takahashi, F.; Kinouchi, N.; Saegusa, J.; Seki, A.; Takemiya, H.; Shibata, T. Detailed Deposition Density Maps Constructed by Large-Scale Soil Sampling for Gamma-Ray Emitting Radioactive Nuclides from the Fukushima Dai-ichi Nuclear Power Plant Accident. *J. Environ. Radioact.* **2015**, *139*, 308−319.
(50) IAEA. Environmental Transfer of Radionuclides in Japan Following the Accident at the Fukushima Daiichi Nuclear Power Plant. *IAEA-TECDOC-1927*. 2020.
(51) Mück, K.; Roth, K.; Gerzabek, M. H.; Oberländer, H. E. Effective Half-Lives of I- and Cs-Isotopes in Grassland Shortly after Fallout. *J. Environ. Radioact.* **1994**, *24*, 127−143.
(52) Winiarek, V.; Bocquet, M.; Saunier, O.; Mathieu, A. Estimation of Errors in the Inverse Modeling of Accidental Release of Atmospheric Pollutant: Application to the Reconstruction of the Cesium-137 and Iodine-131 Source Terms from the Fukushima Daiichi Power Plant. *J. Geophys. Res. Atmos.* **2012**, *117*, 1−16.
(53) Yoshihara, T.; Matsumura, H.; Hashida, S. N.; Nagaoka, T. Radiocesium Contaminations of 20 Wood Species and the Corresponding Gamma-Ray Dose Rates around the Canopies at 5 Months after the Fukushima Nuclear Power Plant Accident. *J. Environ. Radioact.* **2013**, *115*, 60−68.
(54) Kato, H.; Onda, Y.; Wakahara, T.; Kawamori, A. Spatial Pattern of Atmospherically Deposited Radiocesium on the Forest Floor in the Early Phase of the Fukushima Daiichi Nuclear Power Plant Accident. *Sci. Total Environ.* **2018**, *615*, 187−196.

(55) Ould-Dada, Z.; Copplestone, D.; Toal, M.; Shaw, G. Effect of Forest Edges on Deposition of Radioactive Aerosols. *Atmos. Environ.* **2002**, *36*, 5595−5606.
(56) Malins, A.; Imamura, N.; Niizato, T.; Takahashi, J.; Kim, M.; Sakuma, K.; Shinomiya, Y.; Miura, S.; Machida, M. Calculations for Ambient Dose Equivalent Rates in Nine Forests in Eastern Japan from ^{134}Cs and ^{137}Cs Radioactivity Measurements. *J. Environ. Radioact.* **2021**, *226*, No. 106456.
(57) Kato, H.; Onda, Y.; Saidin, Z. H.; Sakashita, W.; Hisadome, K.; Loffredo, N. Six-Year Monitoring Study of Radiocesium Transfer in Forest Environments Following the Fukushima Nuclear Power Plant Accident. *J. Environ. Radioact.* **2019**, *210*, 105817.
(58) Teramage, M. T.; Onda, Y.; Kato, H.; Gomi, T. The Role of Litterfall in Transferring Fukushima-Derived Radiocesium to a Coniferous Forest Floor. *Sci. Total Environ.* **2014**, *490*, 435−439.
(59) Ota, M.; Koarashi, J. Contamination Processes of Tree Components in Japanese Forest Ecosystems Affected by the Fukushima Daiichi Nuclear Power Plant Accident ^{137}Cs Fallout. *Sci. Total Environ.* **2022**, *816*, No. 151587.
(60) Nishikiori, T.; Watanabe, M.; Koshikawa, M. K.; Takamatsu, T.; Ishii, Y.; Ito, S.; Takenaka, A.; Watanabe, K.; Hayashi, S. Uptake and Translocation of Radiocesium in Cedar Leaves Following the Fukushima Nuclear Accident. *Sci. Total Environ.* **2015**, *502*, 611−616.
(61) Calmon, P.; Gonze, M. A.; Mourlon, C. Modeling the Early-Phase Redistribution of Radiocesium Fallouts in an Evergreen Coniferous Forest after Chernobyl and Fukushima Accidents. *Sci. Total Environ.* **2015**, *529*, 30−39.
(62) Kaneyasu, N.; Ohashi, H.; Suzuki, F.; Okuda, T.; Ikemori, F. Sulfate Aerosol as a Potential Transport Medium of Radiocesium from the Fukushima Nuclear Accident. *Environ. Sci. Technol.* **2012**, *46*, 5720−5726.
(63) Miyamoto, Y.; Yasuda, K.; Magara, M. Size Distribution of Radioactive Particles Collected at Tokai, Japan 6 Days after the Nuclear Accident. *J. Environ. Radioact.* **2014**, *132*, 1−7.
(64) Hososhima, M.; Kaneyasu, N. Altitude-Dependent Distribution of Ambient Gamma Dose Rates in a Mountainous Area of Japan Caused by the Fukushima Nuclear Accident. *Environ. Sci. Technol.* **2015**, *49*, 3341−3348.
(65) He, Q.; Walling, D. E. Interpreting Particle Size Effects in the Adsorption of 137Cs and Unsupported ^{210}Pb by Mineral Soils and Sediments. *J. Environ. Radioact.* **1996**, *30*, 117−137.
(66) Nimis, P. L. Radiocesium in Plants of Forest Ecosystems. *Stud. Geobot.* **1996**, *15*, 3−49.
(67) Quérel, A.; Quélo, D.; Roustan, Y.; Mathieu, A. Sensitivity Study to Select the Wet Deposition Scheme in an Operational Atmospheric Transport Model. *J. Environ. Radioact.* **2021**, *237*, No. 106712.

https://doi.org/10.1021/acs.est.2c03451
Environ. Sci. Technol. 2022, 56, 15541−15551